

An experimental and computational study of tip clearance effects on a transonic turbine stage

Adam J. Jackson^{a,*}, Andrew P. S. Wheeler^b, Roger W. Ainsworth^a

^a*Department of Engineering Science, University of Oxford, UK*

^b*Department of Engineering, University of Cambridge, UK*

Abstract

This paper describes an experimental and computational investigation into the influence of tip clearance on the blade tip heat load of a high-pressure (HP) turbine stage. Experiments were performed in the Oxford Rotor facility which is a $1\frac{1}{2}$ stage, shroudless, transonic, high pressure turbine. The experiments were conducted at an engine representative Mach number and Reynolds number. Rotating frame instrumentation was used to capture both aerodynamic and heat flux data within the rotor blade row. Two rotor blade tip clearances were tested (1.5 % and 1.0 % of blade span). The experiments were compared with computational fluid dynamics (CFD) predictions made using a steady Reynolds-averaged Navier–Stokes (RANS) solver. The experiments and computational predictions were in good agreement. The blade tip heat transfer was observed to increase with reduced tip gap in both the CFD and the experiment. The augmentation of tip heat load at smaller clearances was found to be due to the ingestion of high relative total temperature fluid near the casing, generated through casing shear.

Keywords: tip leakage flow, heat transfer, transonic turbine

Nomenclature

C_{ax} Axial chord

C_f Skin friction coefficient

c_p Specific heat capacity at constant pressure

g Tip gap height

h Heat transfer coefficient

M Mach number

\dot{m} Mass flow rate

P Pressure

*E-mail: adam.jackson@eng.oxon.org. Telephone: +447986711780.

\dot{q} Surface heat transfer rate per unit area

T Temperature

U Casing velocity

V Tip flow velocity

x Tip gap width

ρ Density

τ_w Wall shear stress

Subscripts

LG Large gap

1 Stage inlet

2 NGV exit

aw Adiabatic wall

o Stagnation quantity

rel Relative quantity

w Wall

1. Introduction

Turbine blade tips are difficult to cool and, due to their immersion in hot gases, they are susceptible to thermal degradation. A large number of studies have investigated the nature of heat transfer to turbine blade tips. However only a small subset of those studies have performed experiments at fully engine representative flow conditions due to the complexities of rotating-frame testing at engine-scale Mach and Reynolds numbers. The majority of the experiments that have been reported to date have been performed in stationary cascades. At low speed, the heat transfer distribution is dominated by separation of fluid from the pressure side tip gap corner and its possible subsequent reattachment (see for instance [1, 2, 3]).

Newton et al. (2006) [1] used a low speed linear cascade, without relative casing motion, to obtain heat transfer coefficient distributions on the flat tip of a generic turbine blade in a five blade linear cascade. From the two tip gaps (1.6 % and 2.8 % of blade chord) that were tested it was evident that with the larger clearance gap the region of separation increased. The maximum heat transfer coefficient occurred in the region of reattachment on the blade tip — essentially along a line parallel to the pressure side corner. This region was more extensive for the larger tip gap, though the peak heat transfer coefficient values were similar.

Palafox et al. (2006) [2] made similar observations at tip clearances of 1 %, 1.5 % and 3 % of blade chord in a low speed linear cascade; for each tip gap there was a thin region, between mid-chord and the trailing edge, of high Nusselt numbers parallel to the pressure side tip gap corner. As the tip gap was reduced, the high Nusselt number region moved towards the pressure surface

and (in contrast to some other studies, a number of which are discussed below) the Nusselt numbers increased. This trend was the same both with, and without, relative over-tip casing motion. Blade tip static pressure measurements and two-dimensional particle image velocimetry of flow within the tip gap revealed that the high Nusselt number region was associated with the reattachment of the flow that had separated off the sharp pressure side tip gap corner.

Several studies have demonstrated that the flow within the tip gap of a transonic turbine is itself transonic [4, 5, 6]. Numerical simulations and experiments that have reproduced such conditions (by, for instance, using high speed linear cascades) have shown that as well as the separation and subsequent reattachment observed at low speed, blade tip heat transfer distributions may be significantly altered by changes of adiabatic wall temperature and by the reflection of shock waves from the blade tip [7, 8, 9, 10]. These effects may be expected to affect how the heat transfer distributions change when the tip gap is reduced.

Bunker et al. (2000) [11] measured heat transfer coefficient distributions on a flat blade tip downstream of a casing step in a linear cascade with an exit Mach number of 0.75. Decreasing the tip clearance by 37 % (from the nominal tip clearance of 2.0 % of blade span) resulted in approximately a 10 % decrease of heat transfer coefficient, while an equivalent increase of tip clearance resulted in a 10 % increase of heat transfer coefficient.

Azad et al. (2000) [12, 13] made heat transfer measurements on a flat blade tip and recessed tip with tip gaps of 1.0 %, 1.5 % and 2.5 % of blade span in a linear cascade with an exit Mach number of 0.59. It was concluded that generally a larger tip gap resulted in a higher heat transfer coefficient.

Similarly, Nasir et al. (2004) [14] detailed heat transfer coefficient distributions on the tip surface of flat and recessed high pressure turbine blade tips in a linear cascade with an exit Mach number of 0.54. The plain tip exhibited relatively low heat transfer coefficients downstream of the leading edge for both tip gap sizes (1.0 % and 2.6 % of span) due to the low pressure gradient across this area. Flow separation occurred at the pressure side blade tip corner as the flow entered the tip gap and then reattached on the tip surface causing a low heat transfer region immediately downstream of the corner and high heat transfer in the reattachment region. Lower heat transfer coefficients were measured for the smaller tip gap height (1.0 % of blade span) and this was said to be due to the fact that there was less leakage flow over the blade tip than with the larger tip gap (2.6 % of blade span). The enhanced heat load for the larger clearance gap was also attributed to the larger tip gap Reynolds number.

There have also been several studies of blade tip heat transfer made using high speed rotating rigs which more closely simulate the flow conditions found in operational gas turbines [15]. One such example is the study reported by Metzger et al. (1991) [16] who measured blade tip heat transfer rates at five locations that were distributed along the tip between about 5 % and 30 % of chord. The measurements were performed using miniature platinum thin-film gauges at two different tip gaps (0.38 mm and 0.64 mm) using a high speed, rotating, single stage turbine. The results showed an increase of local heat flux of approximately 30 % at about 30 % of blade chord when the tip gap was increased.

Dunn et al. (1984) [17] reported the results of heat flux measurements made on a turbine blade and casing in a high speed full stage rotating turbine. The tip gap was reported to be 0.3 mm when the turbine was operating at 27000 rpm [18]. Ameri and Steinthorsson (1996) [19] modelled the experiment reported in [17] using a code which solved the Reynolds-averaged Navier–Stokes (RANS) equations. This paper is of additional interest because it was reported that the casing and tip measurements were actually conducted for two tip gap heights; 1.11 % and 1.85 % of span at the location of the blade leading edge at the hub (only results from one

tip gap height were reported in [17]). A comparison of the predicted blade tip Stanton number contours (based on inlet conditions and therefore proportional to local heat flux) for the two gap sizes revealed a general decline in levels with increasing tip gap size. This was in agreement with the experimental data which, over the first 30 % of the blade axial chord at the tip, also showed a lower Stanton number when the tip gap was increased. This trend contrasts with many of the cascade based investigations of which some were mentioned previously.

Ameri et al. (1999) [20] performed a numerical study (using a RANS solver and a $k-\omega$ turbulence model without wall functions) of the effects of tip gap height and casing recesses on heat transfer and stage efficiency in a high speed axial turbine. Tip gap heights of 0 %, 1 %, 1.5 %, and 3 % of the passage height were modelled. For the two largest tip gap heights considered, different casing recess depths were studied. The results from the plain casing tests showed that larger tip gap heights increased the predicted Stanton numbers (based on inlet conditions) over the forward half of the blade tip. The converse was true for the aft half of the blade tip. The reason for this was concluded to be that as the clearance was increased the velocity over the upstream portion of the blade tip increased resulting in an increase of heat transfer to the blade tip. The heat transfer to the downstream portion of the blade tip was mostly dominated by the size and the extent of the separation bubble; as the gap was increased there was a larger portion of the blade tip over which the flow was unattached. This led to smaller heat transfer rates to the downstream portion of the blade tip. Nevertheless it was stated that an increase in the thermal load on all the heat transfer surfaces considered was observed due to enlargement of the tip gap.

The effects of endwall motion have been studied predominantly computationally, and tend to show a reduction in over-tip leakage and reduction in heat load [21, 22]. Recent work such as Zhou et al. (2012) [23], showed that both the tip flow aerodynamics and heat flux distribution change significantly with the introduction of a moving endwall. Coull and Atkins (2013) [24] showed recently that the combined effects of a moving casing, and realistic inlet boundary layers and secondary flows entering the rotor passage have a much greater influence on the tip flow and heat transfer than would result from a simple addition of these effects. That is to say that there is a strong coupling between the development of the secondary flows and the endwall motion which has a large influence on the blade tip.

The general consensus from cascade experiments is that reducing tip gap size tends to reduce blade tip heat load. In contrast, those experiments that have been conducted in high speed or rotating facilities have not revealed a general trend in terms of the sensitivity of tip heat load to tip gap size. This paper aims to further improve the understanding of the effect of the tip gap size on both blade tip heat transfer rates and stage aerodynamics at fully engine scaled flow conditions. This will be accomplished by reporting the results of blade tip heat transfer and aerodynamic measurements made in a transonic turbine stage at two different tip gap sizes and comparing these data with computational predictions.

2. Experimental setup

2.1. The Oxford Rotor Facility

Experiments were carried out in the Oxford Rotor Facility (ORF) which is a $1\frac{1}{2}$ stage, shroudless, high pressure, transonic turbine operating at engine representative Mach and Reynolds numbers [25, 26]. The working section, figure 1, consists of 36 high pressure nozzle guide vanes (NGVs), 60 high pressure rotor blades (HPBs) with a rotational speed of 8910 rpm, and 21 intermediate pressure vanes (IPVs) which are located in a swan-necked exit diffuser. The geometry

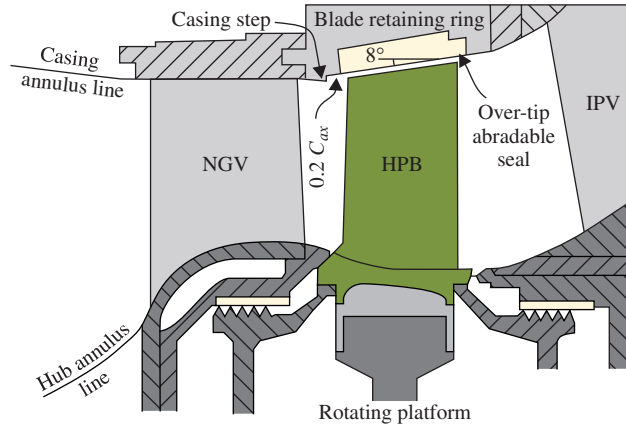


Figure 1: Schematic showing the stage geometry of the large and small gap builds.

is representative of that found in a large civil turbofan aero-engine. Isentropically compressed air is provided to the working section for a period of approximately 200 ms by means of an isentropic light piston tunnel (ILPT) [27]. For the experiments described in this paper, the stage inlet stagnation pressure and temperature were 8.04 bar and 374.4 K. The conditions at NGV exit were a Mach number of 0.94 and a Reynolds number of 2.7×10^6 (based on conditions at mid-height and vane axial chord). As with previous experiments conducted using the ORF the realised relative frame gas-to-wall temperature ratio for the blade was typically 1.07.

2.1.1. Stage geometry

The geometry of the ORF working section included a backwards facing casing step 20 % of HPB axial chord upstream of the leading edge of the rotor (figure 1). The 1.2 mm high casing step was intended to have a height equal to the tip gap [28]. This configuration will be referred to as the ‘large gap’ build.

In this study modifications were made to the working section so as to provide an extra test case with a different tip gap: the ‘small gap’ build. In contrast to the conventional approach of grinding down the HPBs to increase the tip gap, in this study the mean tip gap was reduced from its initial large value by modifying the over-tip casing. This was done without disassembling the NGV, HPB, or IPV rings so that their throat areas were not inadvertently altered nor was the clocking of the NGV and IPV rings changed.

Figure 2 shows a comparison of the measured tip gap around the annulus before and after the over-tip casing abrasible seal was modified. Small discontinuities were found at the interfaces between the blade retaining rings and removable instrumentation cassettes (20°, 160°, 200° and 340°) and at the interfaces between the removable instrumentation module and over-tip casing instrumentation block (170° and 190°). **A small variation in tip clearance of approximately ± 0.25 mm was also found around the annulus. This was greatly reduced with the modified casing.**

The effect of the small circumferential non-uniformity was investigated both experimentally and computationally. Experimentally, the time-resolved data were conditionally averaged over two different sectors of the annulus each of which had different mean tip gaps as a consequence of

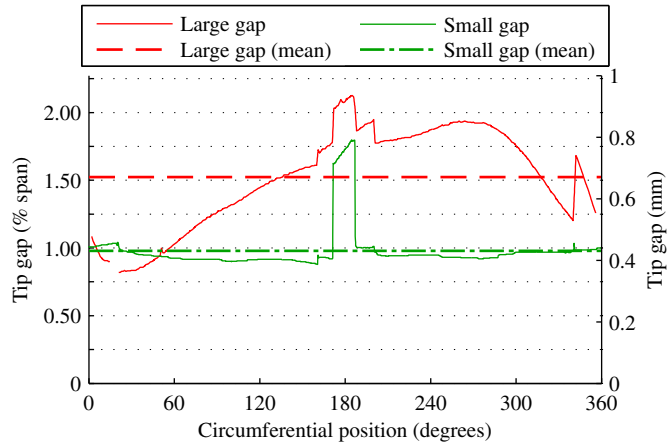


Figure 2: Comparison of axial mean tip gaps between large gap and small gap builds. A correction for disc growth has been included. Circumferential position was measured anti-clockwise from the horizontal.

the small circumferential variation shown in figure 2. The two sectors each spanned 18 complete, unique and contiguous NGV passages, and were chosen such that the difference in mean tip gap between sectors was maximised. Computationally, a deforming mesh was used to simulate the radial motion of the casing relative to the tip; these were transient calculations in which the tip gap was changing dynamically. Both experimental and computational results were found to be consistent with both time-averaged experimental data and steady CFD results. This demonstrates that the tip boundary layer responds in a quasi-steady way to the long length scale circumferential non-uniformity.

Figure 2 also shows a comparison of the mean tip gap for each build. The large gap build had an average measured clearance of 1.5 % span, and the small gap build had a clearance of 1.0 % span (based on the HPB span at mid axial chord being equal to 44 mm).

2.2. Measurement techniques

All electrical connections to the rotating frame instrumentation were made via a 24 channel slip ring. Both DC and amplified AC coupled signals were sampled to minimise digitisation error. The signals were sampled by a 12-bit analogue-to-digital converter at 500 kHz with a 100 kHz anti-aliasing filter being applied prior to sampling.

2.2.1. Heat transfer rate instrumentation

Extensive details of the theory of operation of the thin film resistance thermometers used herein and the signal processing techniques necessary for their operation have been reported previously [29, 30] and only a brief summary is given here.

Thin film resistance thermometers, or thin film gauges (TFGs) as they will be referred to, operate on the principle that heat transferred through the TFG into the substrate causes the TFG and the substrate to change temperature. The relationship between the resistance of the platinum film and its temperature is known precisely and time-resolved measurements of the TFG resistance can be used to determine accurately the TFG temperature history. The short duration of measurements in the ORF prevent heat entering through the blade tip from being conducted to the other

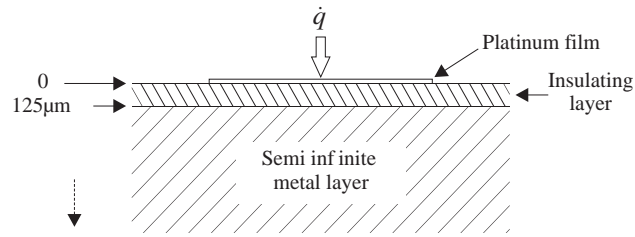


Figure 3: Schematic cross section of the two layer substrate gauge, adapted from Ainsworth et al. (1989) [30].

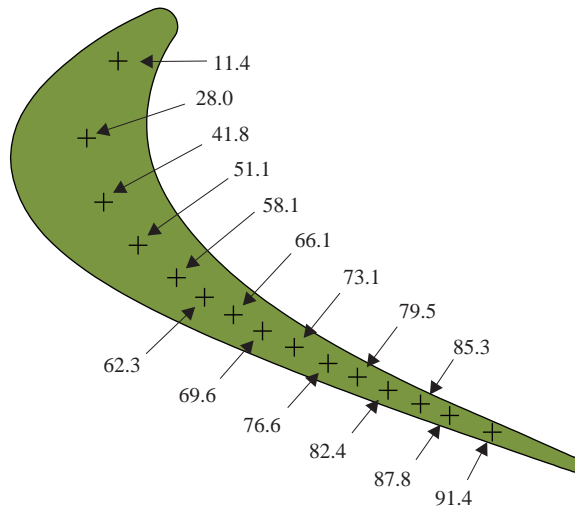


Figure 4: Positions of camber line TFGs. Numbers indicate gauge positions as a percentage of axial chord.

boundaries of the blade. The metal layer can therefore be treated as being semi-infinite and the governing equations solved to yield the time-resolved heat transfer rate at the gauge location. A cross section of a ‘two layer substrate gauge’, in which the platinum film is electrically isolated from the semi-infinite metal layer by means of an electrical insulator, is shown schematically in figure 3.

Thorpe et al. (2000, 2004) [31, 32] produced the blade tip mounted TFGs using a laser machining technique. The 1 mm by 0.08 mm TFGs, oriented with their long axis tangent to the camber line, each consisted of a 0.1 μm thick platinum film deposited on an insulating layer of vitreous enamel approximately 125 μm thick which covered a blade made of Inconel718. The thermal capacity of the film was extremely small in comparison to that of the substrate. The locations of the TFGs mounted along the blade tip are illustrated in figure 4. Electrical connections to each TFG were made by gold plated copper tracks which had resistances of less than 1 % of the resistances of the TFGs.

2.2.2. Heat transfer rate measurements

The stage inlet total temperature, T_{o1} , and wall temperature, T_w , varied by several kelvins between test runs due to small differences in the initial conditions within the ILPT prior to a run and changes in ambient conditions. These changes affected the driving temperature difference between the gas and the metal and thus a correction was applied to the measured heat transfer rates to avoid incurring a systematic error when comparing different sets of data. The correction was as follows:

$$\dot{q}_c = \dot{q} \frac{\overline{T_{o2,rel}} - \overline{T_w}}{\overline{T_{o2,rel}} - T_w + (T_{o1} - \overline{T_{o1}})} \quad (1)$$

where T_w and T_{o1} were the measured quantities during a run and $\overline{T_{o1}}$, $\overline{T_{o2,rel}}$ and $\overline{T_w}$ were the nominal design-point values (i.e., 374.4 K, 328 K and 304 K respectively). The measured wall temperature was calculated from the sum of the TFG temperature immediately before gas began to flow through the working section and the temperature rise of the TFG due to the working fluid.

2.2.3. Aerodynamic measurements

A series of aerodynamic measurements were made in conjunction with the detailed heat transfer investigation. Blade-surface mounted Kulite pressure gauges [33] were used to measure static pressures at three locations on the blade tip (at 11.7 %, 31.7 %, and 55.1 % C_{ax} respectively) and relative total pressure on the HPB leading edge at 90 % of HPB leading edge span.

2.3. Uncertainty estimates

The measurement uncertainty in heat transfer rate is estimated to be ± 5 % [34]. The precision of the measurements is indicated by the error bars showing the standard error of the mean for the data obtained using the small gap build (the precision of the data obtained using the large gap build would be expected to be similar). Ainsworth et al. (2000) [35] conducted a thorough analysis of the measurement errors incurred when using the Kulite semiconductor pressure transducer in this application. The calibration uncertainty was predicted to be less than 0.2 %. The resistances of the diffused resistors which made up the static pressure gauge varied with temperature. According to [35] the trueness uncertainty in static pressure was 0.066 % per kelvin. The blade tip heat transfer measurements showed that the largest temperature rise was 11 K on the blade tip. The overall uncertainty in the static pressure measurements was therefore 0.8 % ± 0.2 % [trueness \pm precision], as in keeping with previous experiments the static pressure measurements made in this study were not compensated for changing gauge temperatures.

3. Computational set-up

Computational predictions were performed using the ANSYS-CFX 14.5 solver. Computational grids of the stage including the NGV and HPB were created using the ANSYS Turbogrid software. An example of the grids used is shown in figure 5. The spanwise distribution of 100 mesh lines in the tip gap gave a wall y^+ of the first grid point away from the wall of less than 2 over the tip surface. A fillet of 0.2 mm radius was also included so as to match the geometry tested in the experiment. Experimentally determined boundary conditions were used to match the experimental operating point. Isothermal walls were set on the HPB surface; data was obtained at two wall temperatures of 304 K and 315 K in order to obtain the heat transfer coefficient, $h = \Delta\dot{q}/\Delta T_w$, and adiabatic wall temperature, $T_{aw} = \dot{q}/h + T_w$. The $k - \omega$ SST turbulence model

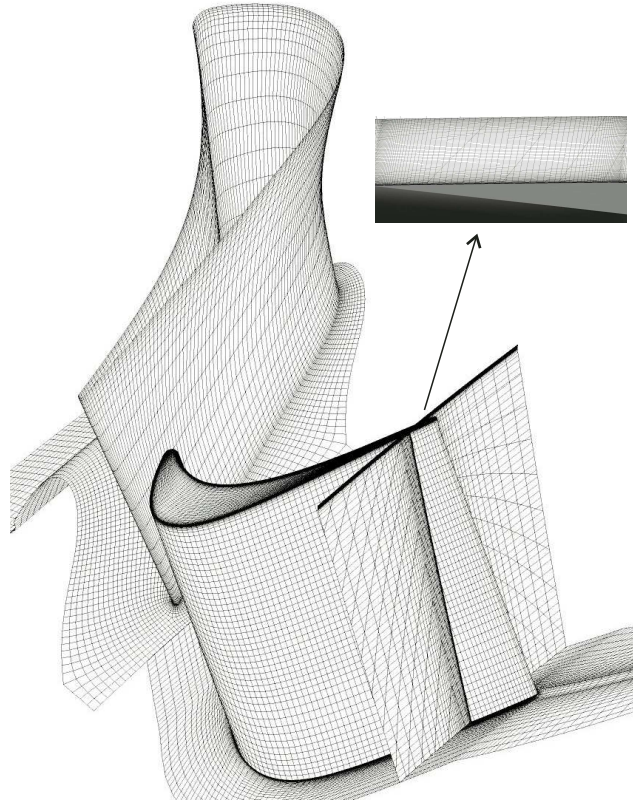


Figure 5: Example of computational mesh used showing detail in tip region.

was used with the $\gamma - \theta$ transition model; this choice was based on previous DNS data from [36] which showed that the $k - \omega$ SST model gives a reasonable prediction of reattachment-point heat transfer in the case of a transonic tip flow where high levels of free-stream turbulence are likely. A mixing-plane between stator and rotor rows was implemented in order to circumferentially average the flow entering the rotor, and therefore enable the use of steady-state CFD.

Several different computational meshes were tested to determine the resolution required for mesh independence. The tip heat load was not found to vary significantly for grid sizes above 2 million cells, with 100 spanwise cells in the tip gap (see figure 6). **The y^+ of the first grid point away from the tip was between 1 and 3, with a mean value of 2 whilst the remainder of the blade had an average y^+ of 3. This was considered sufficient to ensure resolution of the viscous sub-layer and is consistent with recent aerodynamic work of Schabowski et al. (2014) [37] (tip $y^+ \approx 4$) and aerothermal work of Viridi et al. (2015) [38] (tip y^+ largely between 1 and 3) who demonstrated close agreement between CFD and experiment.**

4. Results

Figure 7 shows the experimentally measured tip surface heat flux along the camber line. Data is shown for both the large gap (1.5 % span) and small gap (1.0 % span) cases. The results show a

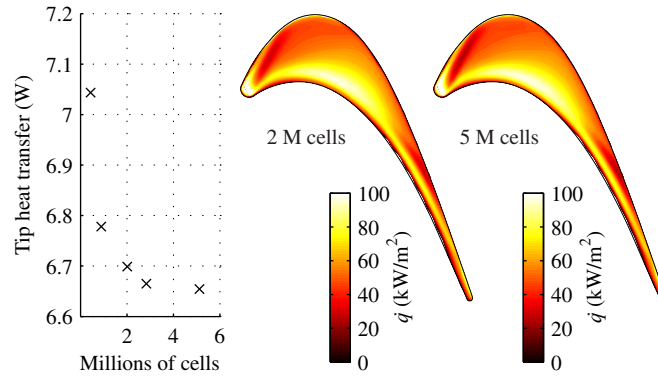


Figure 6: Variation of tip heat load with mesh size.

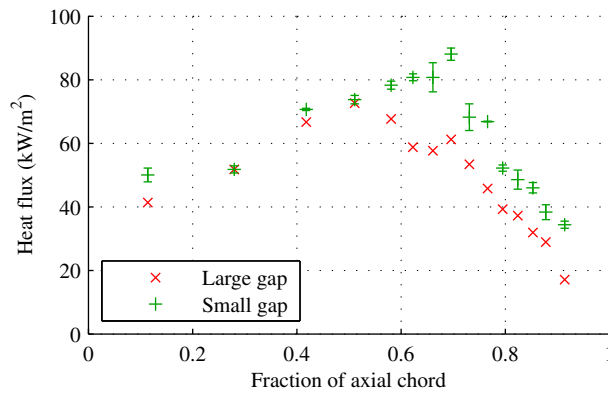


Figure 7: Experimentally measured heat flux along blade tip camber line.

large increase in the measured heat load at the smaller tip clearance, particularly in the aft region of the tip. The peak heat load rises by around 30 %, and shifts downstream from around $0.5 C_{ax}$ to $0.7 C_{ax}$, as the clearance is reduced from 1.5 to 1.0 % span. The cause of this rise is interesting since previous work, particularly in subsonic cascades, has often indicated that reducing the tip gap causes a reduction of heat transfer coefficient and by implication heat transfer rate (section 1).

In order to understand further the factors influencing the tip heat load, it is useful to introduce the results from the computational simulations and compare these with the experimental data. A comparison of the predicted loading distributions with previous experimental data are shown in figure 8. The peak Mach numbers in the HPB are under predicted by the CFD, while for the NGV the agreement between CFD and experiment is generally good. The effect of tip clearance on the predicted loading can also be observed by comparing the large gap and small gap results; these show that the reduction in tip clearance increases the blade loading slightly whilst reducing the NGV loading. The increased blade loading is consistent with the reduction in tip leakage flow expected for the smaller tip clearance case, since the reduction in over-tip leakage will increase the overall turning of the flow, and therefore must be accompanied by an increase in blade loading. Since the overall total-to-static pressure ratio across the stage is fixed, this has the effect of also reducing the NGV loading. The change in NGV loading affects the driving

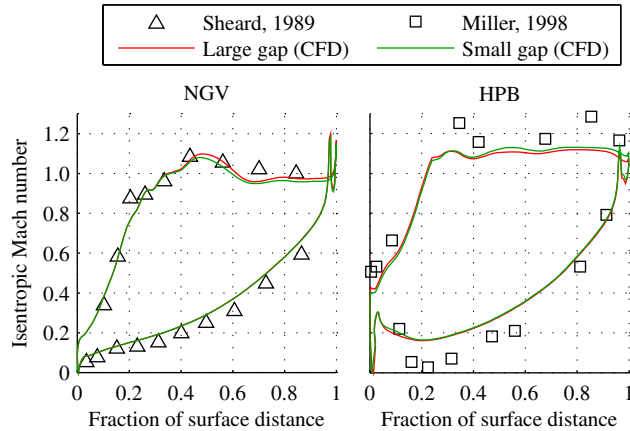


Figure 8: Comparison of mid-span isentropic Mach numbers predicted by the CFD with experimental data from [39, 40].

temperature difference which in turn affects the blade heat transfer, and this is discussed in more detail later.

A comparison of the measured tip surface static pressure along a camber line with CFD predictions is shown in figure 9. The predictions compare well with measurements, showing a large drop in static pressure over the aft region of the tip consistent with the large blade loading in this region (see also figure 8).

Before discussing the tip heat transfer, it is useful to identify the Mach number within the tip gap since previous work shows that the blade tip heat transfer and flow structure of a supersonic tip flow differ considerably from a subsonic tip flow [7, 9, 10]. Figure 10 shows the isentropic Mach number in the tip gap (calculated using the tip surface static pressure); these data can be used to determine the extent of supersonic flow in the tip gap. A contour line is shown to identify the $M = 1$ boundary; fore of this line is the subsonic region (labelled region A), and aft of this line is the supersonic region (labelled B). Reducing the tip gap from 1.5 to 1.0 % span has the effect of both reducing the region of supersonic flow (region B) and also reducing the peak Mach number by about 10 %. This is important because the tip Mach number affects both the heat transfer coefficient and adiabatic wall temperature [7].

The predicted tip surface heat flux is shown in figure 11 for the large gap and small gap cases. In both cases the subsonic region (A) of the tip flow tends to experience higher heat flux levels compared with the supersonic region (B), consistent with previous results [7, 9, 10]. The figure shows a high heat flux region near the pressure side edge, corresponding with the reattachment-line of the separation bubble in this region. The reduction in clearance also leads to a shift in the reattachment location towards the pressure side edge. The results show that the reattachment-point heat flux rises by around 10 %, and the total tip heat load rises by 5 %, as the tip clearance is reduced from 1.5 to 1.0 % span. As well as the peaks in heat flux near the pressure side edge, there is a local minimum in heat flux near the leading edge (marked C), and a region of elevated heat flux near the suction-side edge marked D, and these will be discussed later. Also shown in the figure are the predicted distributions of heat transfer coefficient and adiabatic wall temperature which will also be discussed later. Before doing so, it is important to establish the veracity of the CFD results by comparing with the experimental data.

A comparison of the predicted tip heat transfer rates with the experimental data measured

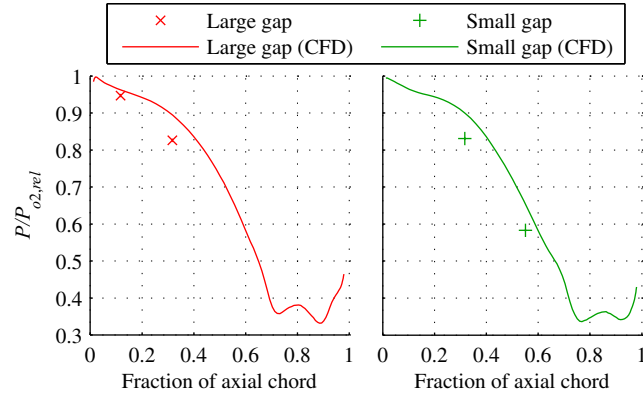


Figure 9: Comparison of experimental measurements of tip surface static pressure (symbols) with the CFD predictions along the blade tip camber line.

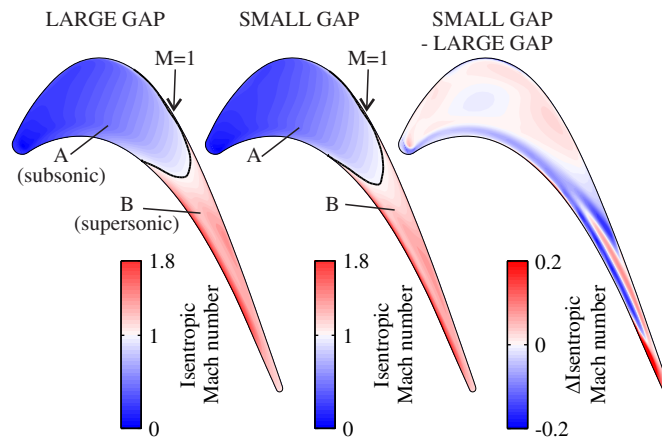


Figure 10: Predicted tip surface isentropic Mach number and change in tip surface isentropic Mach number.

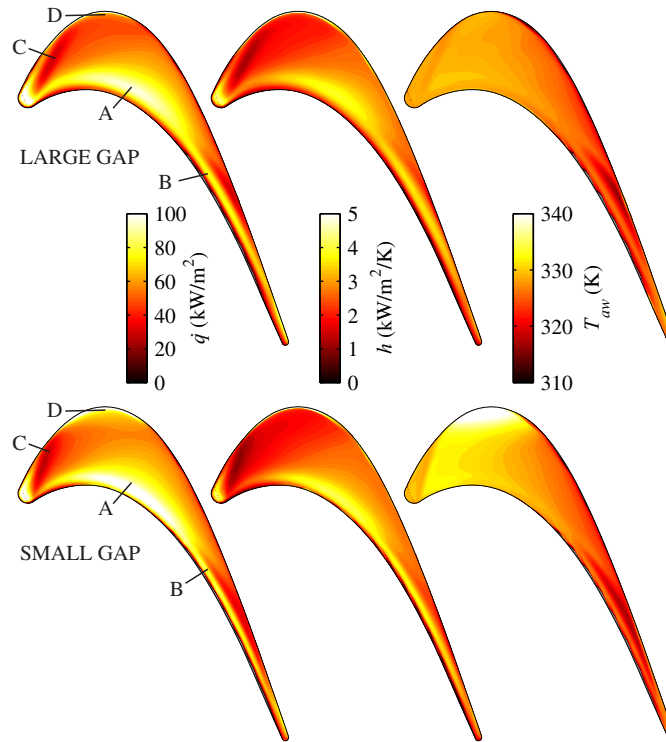


Figure 11: Predicted tip surface heat flux, heat transfer coefficient and adiabatic wall temperature.

along the camber line is shown in figure 12. For the large gap case, the agreement over the first 70 % of axial chord is very encouraging considering the complexity of the flow in this region, and that the CFD predictions do not **model the unsteady vane/rotor interaction**. Over the latter 30 % of axial chord, the predicted heat flux rises sharply due to the separation bubble reattachment which crosses the camber line in this region. CFD data is also shown along a line 30 % of the local tip width displaced from the camber line toward the pressure side edge. Data along this line compares well with the measurements, suggesting that the size of the pressure side edge separation bubble is under predicted by the CFD; this is consistent with previous DNS results (see [36]) which showed that even at engine-scale Reynolds numbers the transonic tip flow is only intermittently turbulent, and consequently RANS predictions of transonic tip flow tend to under predict the separation bubble length. Experimental data for the small gap also compares well with the CFD data extracted along this line, and agrees with the general trend of increased heat flux at the smaller clearance.

The convective heat flux equation, $\dot{q} = h(T_{aw} - T_w)$, shows that the change in heat flux which occurs as tip gap is reduced results from either changes in adiabatic wall temperature or heat transfer coefficient, or a combination of both. The effect of reducing tip clearance on heat transfer coefficient can be seen in figure 11. For the small gap case the heat transfer coefficient at the reattachment point is about 20 % higher as compared to the large gap case. This is consistent with the reduction in Mach number in the region of the bubble reattachment which occurs in the small gap case since, as previous work shows, a reduction in Mach number tends to increase the

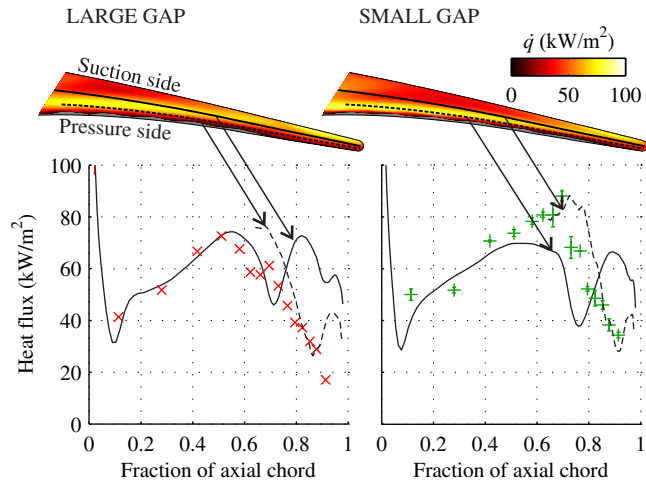


Figure 12: Comparison of experimentally measured heat flux (symbols) with the CFD predictions. CFD data were extracted along the camber line, and a line 30 % of the tip width offset from the camber line towards the pressure surface.

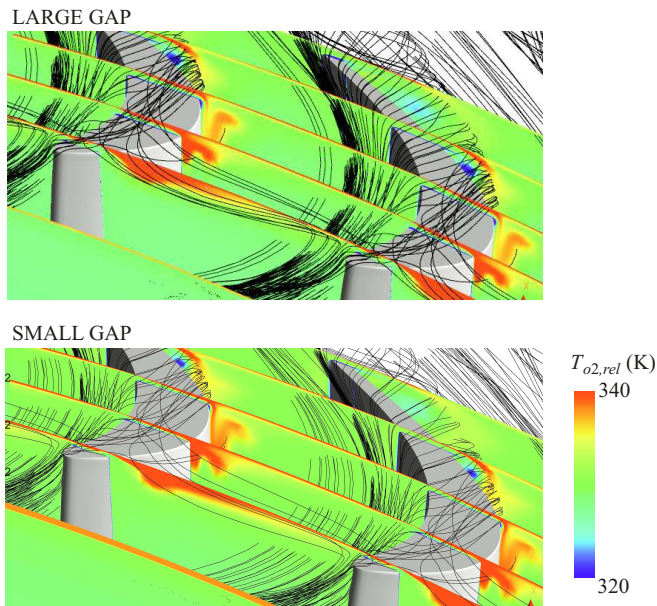


Figure 13: Predicted relative total temperature and streamline pattern near to the tip.

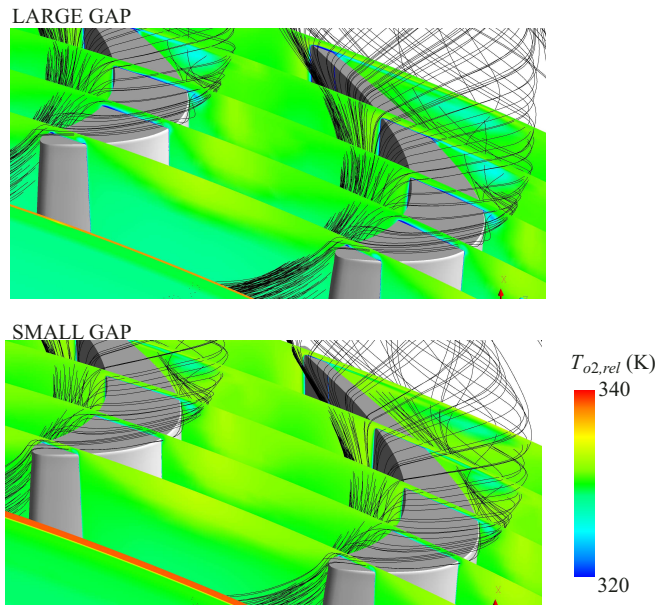


Figure 14: Predicted relative total temperature and streamline pattern near to the tip with a slip-wall casing.

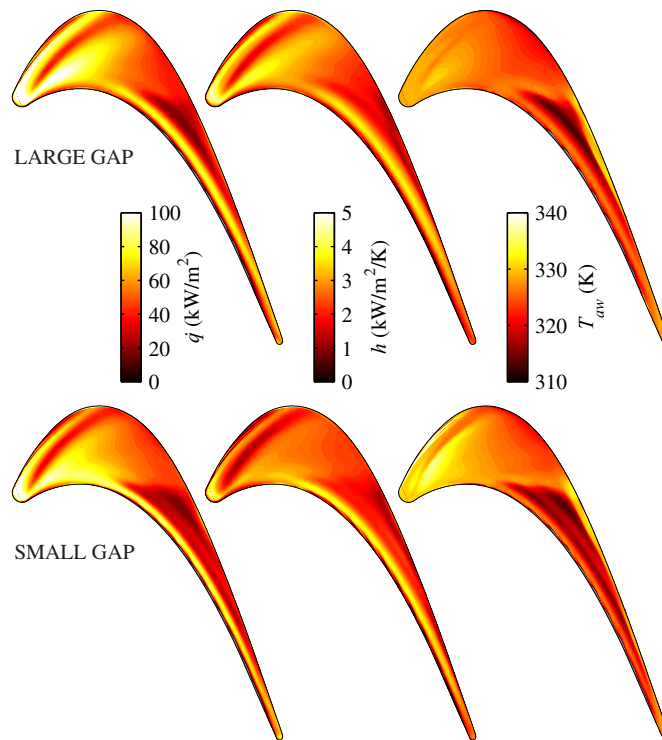


Figure 15: Predicted tip surface heat flux, heat transfer coefficient and adiabatic wall temperature with a slip-wall casing.

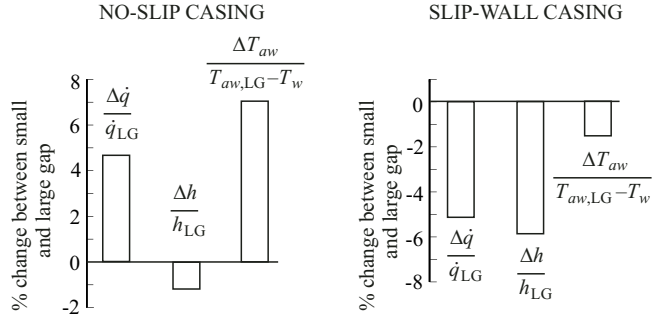


Figure 16: Predicted change in the area-averaged heat flux, heat transfer coefficient and driving temperature difference over the tip surface with and without a slip-wall casing.

turbulence production which occurs in the reattachment [7]. However, away from the reattachment regions, the heat transfer coefficient tends to be lower for the small gap case (by around 30 % on average), particularly in region C, where the heat transfer coefficient drops by as much as 50 %.

The effect of reducing tip clearance on the driving temperature difference can also be seen in figure 11. There is a global increase in adiabatic wall temperature as the tip gap is reduced, and this results in an area-averaged change in driving temperature difference of around 6 %. Region D is most affected by the change in clearance, and at this point the local driving temperature difference rises by about 50 %. The changes in adiabatic wall temperature are either due to changes in Mach number (which therefore change the recovery temperature) or are due to changes in the relative total temperature. The area-averaged isentropic Mach number reduces from 0.728 at a gap of 1.5 % span to 0.721 at a gap of 1.0 % span, which is a change of less than 1 % and is not sufficient to account for the global increase in adiabatic wall temperature over the tip surface at the reduced clearance. The results predicted an increase in mass-averaged relative total temperature at the inlet to the rotor of around 0.25 %, which accounts for a change in driving temperature difference of around 3.5 %; this change in relative total temperature is a consequence of the reduction in NGV loading which occurs as the tip clearance is reduced (see figure 8). The remaining increase in driving temperature difference arises due to the influence of casing shear, as indicated in figure 13. This figure shows the relative total temperature in the tip region as well as the streamlines over the tip; the flow near the casing is a region of elevated relative total temperature which is driven into the tip gap. In the frame of reference of the rotor, the casing boundary layer is subjected to shear work due to the relative motion of the casing, and this raises the relative total temperature of the flow near the casing. This fluid then migrates into the tip under the influence of the cross passage pressure gradient and the wall shear. At the smaller clearance, the high temperature casing boundary layer strongly influences the adiabatic wall temperature in region D, thus leading to the locally elevated driving temperature in this region. Further aft of region D, the leakage jet exits the gap with a higher momentum (because of the increased pressure ratio across the tip), and this prevents ingestion of the casing boundary layer into the tip.

The increased proximity to the tip surface of the casing flow at the reduced clearance is a significant cause of the increase in driving temperature difference for the small gap case, and therefore also a significant cause of the increased tip heat load when the tip gap was reduced. This

was confirmed by performing calculations with a slip-wall condition on the casing, so as to switch off the casing shear. The relative total temperature in the tip region for these calculations is shown in figure 14; this figure clearly shows that the high temperature casing flow is eliminated when the casing shear is removed. The corresponding tip surface heat flux, heat transfer coefficient, and adiabatic wall temperature are shown in figure 15. Comparing figure 15 with figure 11 shows that casing shear has a profound effect on the blade tip heat transfer, in particular in the region near the leading edge. The removal of casing shear changes substantially the distribution of both the heat transfer coefficient and the adiabatic wall temperature; the change to the heat flux is due to changes in both of these quantities. The adiabatic wall temperature is changed because of the removal of the high temperature fluid near the casing, and the heat transfer coefficient is altered largely due to the change in flow pattern over the tip, near the leading edge, as shown by the streamline pattern in figures 13 and 14.

The effect of reducing the tip clearance is changed substantially by the removal of the casing shear in terms of both the distribution of heat load and the average heat load. The area-averaged changes in heat flux, heat transfer coefficient and driving temperature difference between the large gap and small gap are shown in figure 16 for the cases with and without casing shear. For the case with casing shear (no-slip casing) the data indicates that the rise in total heat load at the reduced tip clearance is largely due to the change in adiabatic wall temperature, and that there is a small drop in the area-averaged heat transfer coefficient of just over 1 %. In contrast to this, the case with no casing shear (slip-wall casing) shows a 5 % drop in heat load at the smaller clearance, which is primarily due to a reduction in heat transfer coefficient of about 6 %. Thus, the effect of casing shear reverses the sensitivity of the heat load to tip clearance. The imposition of casing shear reduces the change in heat transfer coefficient between the large gap and small gap cases, and also introduces the additional effect of shear work which raises the relative total temperature of the over-tip flow when the tip clearance is reduced.

Finally, it is important to consider to what extent the influence of casing shear may differ between high speed and low speed experiments. An energy balance in the frame of reference of the blade tip shows that the proportional change in driving temperature difference due to casing shear is proportional to the casing skin friction coefficient and the square of the casing Mach number. This can be deduced with reference to figure 17 in which a plane parallel to the tip gap flow is illustrated. Assuming adiabatic walls, the change in energy of fluid flowing through the tip gap (say between the inlet, A, and exit, B) can be equated to the shear work done on the fluid by the casing. For unit distance normal to the plane we then have:

$$\begin{aligned} \dot{m} \cdot c_p \cdot \Delta(T_{o2,rel} - T_w) &= \tau_w \cdot x \cdot 1 \cdot U \\ &= \frac{C_f}{2} \rho (U + V)^2 \cdot x \cdot 1 \cdot U \end{aligned} \quad (2)$$

where \dot{m} is the mass flow rate through the tip gap, c_p is the specific heat capacity at constant pressure, τ_w is the wall shear stress, x is the distance between the inlet, A, and exit, B, C_f is the casing skin friction coefficient, and U and V are respectively the casing and over-tip flow speeds. The mass flow rate, \dot{m} , on the left hand side of equation 2 can be rewritten as a product of the density and velocity of the fluid flow, the dimensions of the tip gap, and a discharge coefficient. By rearranging and cancelling terms we then see that

$$\frac{\Delta(T_{o2,rel} - T_w)}{(T_{o2,rel} - T_w)} \propto \frac{C_f}{2} \left(\frac{(U + V)^2}{T_{o2,rel}} \right) \left(\frac{1}{1 - \frac{T_w}{T_{o2,rel}}} \right) \frac{U \cdot x}{V \cdot g} \quad (3)$$

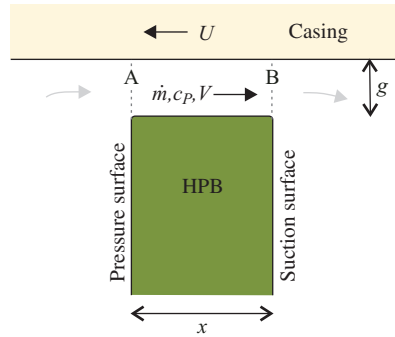


Figure 17: Two-dimensional tip analysis. In the frame of reference of the blade tip the fluid in the tip gap has a velocity V , and the casing has a velocity $-U$.

where g is the height of the tip gap. The second term on the right hand side is effectively a Mach number scaling; higher Mach numbers will lead to proportionally larger changes in driving temperature difference.

5. Conclusions

In this paper the effects of tip clearance on blade tip heat load were investigated experimentally and computationally. Experiments were performed within a transonic turbine, matching engine-scale non-dimensional conditions. CFD calculations were also performed and the results compared favourably with the experimental data; both sets of data showed a tendency for heat load to rise as clearance was reduced from 1.5 to 1.0 % span. A major cause of this was an increase in driving temperature difference observed at smaller clearances resulting from casing shear which locally raised the relative total temperature of the flow near the casing. At smaller clearances, the proximity of this high temperature fluid to the blade tip significantly increased the overall tip heat load. Simulations were performed with casing shear removed (by using a slip-wall on the casing) which confirmed this effect, and also showed that the influence of casing shear greatly modified both the distribution of heat flux over the tip, and also the sensitivity of the tip heat load to tip clearance. Without casing shear, reducing clearance led to a decrease in heat load, largely due to a drop in heat transfer coefficient. With casing shear, the effects of heat transfer coefficient on tip heat load were greatly reduced, and the dominant effect on the total heat load was the influence of adiabatic wall temperature. The results suggest that studies of blade tip heat transfer which do not account for casing shear (i.e. without a moving endwall) may not be reliably used to determine the sensitivity of heat load to tip clearance at engine conditions.

Acknowledgment

The authors gratefully acknowledge the support of Nigel Brett, Pete Fair, Anthony Cooper and others from the Osney Thermo-Fluids Laboratory, University of Oxford. This work was sponsored by Rolls-Royce plc and the Isle of Man Government. The authors wish to thank Rolls-Royce plc for granting permission to publish this work.

- [1] P. J. Newton, G. D. Lock, S. K. Krishnababu, H. P. Hodson, W. N. Dawes, J. Hannis, C. Whitney, Heat transfer and aerodynamics of turbine blade tips in a linear cascade, *Journal of Turbomachinery* 128 (2006) 300–309.

- [2] P. Palafox, M. L. G. Oldfield, P. T. Ireland, T. V. Jones, J. E. LaGraff, Blade tip heat transfer and aerodynamics in a large scale turbine cascade with moving endwall, in: Proceedings of GT2006, ASME Turbo Expo 2006: Power for Land, Sea and Air, May 8–11, 2006, Barcelona, Spain, no. GT2006-90425, 2006.
- [3] S. W. Lee, H. S. Moon, S. E. Lee, Tip gap height effects on flow structure and heat/mass transfer over plane tip of a high-turning turbine rotor blade, *International Journal of Heat and Fluid Flow* 30 (2009) 198–210.
- [4] J. Moore, J. G. Moore, G. S. Henry, U. Chaudhry, Flow and heat transfer in turbine tip gaps, *Journal of Turbomachinery* 111 (1989) 301–309.
- [5] J. Moore, K. M. Elward, Shock formation in overexpanded tip leakage flow, *Journal of Turbomachinery* 115 (1993) 392–399.
- [6] S. J. Thorpe, R. J. Miller, S. Yoshino, R. W. Ainsworth, N. W. Harvey, The effect of work processes on the casing heat transfer of a transonic turbine, *Journal of Turbomachinery* 129 (2007) 84–91.
- [7] A. P. S. Wheeler, N. R. Atkins, L. He, Turbine blade tip heat transfer in low speed and high speed flows, *Journal of Turbomachinery* 133 (2011) 041025–1–041025–9.
- [8] V. Shyam, A. Ameri, J.-P. Chen, Analysis of unsteady tip and endwall heat transfer in a highly loaded transonic turbine stage, Tech. Rep. TM-2010-216740, NASA (2010).
- [9] Q. Zhang, D. O. O’Dowd, L. He, M. L. G. Oldfield, P. M. Ligrani, Transonic turbine blade tip aero-thermal performance with different tip gaps: Part I — Tip heat transfer, *Journal of Turbomachinery* 133 (2011) 041027.
- [10] Q. Zhang, D. O. O’Dowd, L. He, A. P. S. Wheeler, P. M. Ligrani, B. C. Y. Cheong, Overtip shock wave structure and its impact on turbine blade tip heat transfer, *Journal of Turbomachinery* 133 (2011) 041001.
- [11] R. S. Bunker, J. C. Bailey, A. A. Ameri, Heat transfer and flow on the first-stage blade tip of a power generation gas turbine: Part 1 — Experimental results, *Journal of Turbomachinery* 122 (2000) 263–271.
- [12] G. S. Azad, J. Han, S. Teng, R. J. Boyle, Heat transfer and pressure distributions on a gas turbine blade tip, *Journal of Turbomachinery* 122 (2000) 717–724.
- [13] G. S. Azad, J. Han, R. J. Boyle, Heat transfer and flow on the squealer tip of a gas turbine blade, *Journal of Turbomachinery* 122 (2000) 725–732.
- [14] H. Nasir, S. V. Ekkad, D. M. Kontrovitz, R. S. Bunker, C. Prakash, Effect of tip gap and squealer geometry on detailed heat transfer measurements over a high pressure turbine rotor blade tip, *Journal of Turbomachinery* 126 (2004) 221–228.
- [15] R. S. Bunker, A review of turbine blade tip heat transfer, *Annals of the New York Academy of Sciences* 934 (2001) 64–79.
- [16] D. E. Metzger, M. G. Dunn, C. Hah, Turbine tip and shroud heat transfer, *Journal of Turbomachinery* 113 (1991) 502–507.
- [17] M. G. Dunn, W. J. Rae, J. L. Holt, Measurement and analyses of heat flux data in a turbine stage: Part II — Discussion of results and comparison with predictions, *Journal of Engineering for Gas Turbines and Power* 106 (1984) 234–240.
- [18] M. G. Dunn, W. J. Rae, J. L. Holt, Measurement and analyses of heat flux data in a turbine stage: Part I — Description of experimental apparatus and data analysis, *Journal of Engineering for Gas Turbines and Power* 106 (1984) 229–233.
- [19] A. A. Ameri, E. Steinthorsson, Analysis of gas turbine rotor blade tip and shroud heat transfer, in: Proceedings of the International Gas Turbine and Aeroengine Congress and Exhibition, Birmingham, UK — June 10–13, 1996, no. 96-GT-189, 1996.
- [20] A. A. Ameri, E. Steinthorsson, D. L. Rigby, Effects of tip clearance and casing recess on heat transfer and stage efficiency in axial turbines, *Journal of Turbomachinery* 121 (1999) 683–771.
- [21] S. K. Krishnababu, W. N. Dawes, H. P. Hodson, G. D. Lock, J. Hannis, C. Whitney, Aero-thermal investigations of tip leakage flow in axial flow turbines part II — Effect of relative casing motion, in: Proceedings of GT2007, ASME Turbo Expo 2007: Power for Land, Sea and Air, May 14–17, 2007, Montreal, Canada, no. GT2007-27957, 2007.
- [22] J. Tallman, B. Lakshminarayana, Numerical simulation of tip leakage flows in axial flow turbines, with emphasis on flow physics: Part II — Effect of outer casing relative motion, *Journal of Turbomachinery* 123 (2001) 324–333.
- [23] C. Zhou, H. Hodson, I. Tibbott, M. Stokes, Effects of endwall motion on the aero-thermal performance of a winglet tip in a HP turbine, *Journal of Turbomachinery* 134 (2012) 061036.
- [24] J. D. Coull, N. R. Atkins, The influence of boundary conditions on tip leakage flow, in: Proceedings of the ASME 2013 Turbine Blade Tip Symposium. TBTS2013. September 30 – October 3, 2013, Hamburg, Germany, no. TBTS2013-2057, 2013.
- [25] R. W. Ainsworth, D. L. Schultz, M. R. D. Davies, C. J. P. Forth, M. A. Hilditch, M. L. G. Oldfield, A. G. Sheard, A transient flow facility for the study of the thermofluid dynamics of a full stage turbine under engine representative conditions, Tech. Rep. ASME Paper No. 88-GT-144, The American Society of Mechanical Engineers (1988).
- [26] R. J. Miller, R. W. Moss, R. W. Ainsworth, N. W. Harvey, Wake, shock, and potential field interactions in a 1.5 stage turbine — Part I: Vane-rotor and rotor-vane interaction, *Journal of Turbomachinery, Transactions of the ASME* 125

- (2003) 33–39.
- [27] T. V. Jones, D. L. Schultz, A. D. Hendley, On the flow in an isentropic light piston tunnel, Tech. Rep. Aeronautical Research Council Reports and Memoranda No. 3731, Dept. Engineering Science, University of Oxford (1973).
 - [28] G. A. Thomas, N. R. Atkins, S. J. Thorpe, R. W. Ainsworth, N. W. Harvey, The effect of a casing step on the over-tip aerothermodynamics of a transonic HP turbine stage, in: Proceedings of GT2007, ASME Turbo Expo 2007: Power for Land, Sea and Air, May 14–17, 2007, Montreal, Canada, no. GT2007-27780, 2007.
 - [29] J. E. Doorly, Procedures for determining surface heat flux using thin film gages on a coated metal model in a transient test facility, *Journal of Turbomachinery* 110 (1988) 242–250.
 - [30] R. W. Ainsworth, J. L. Allen, M. R. D. Davies, J. E. Doorly, C. J. P. Forth, M. A. Hilditch, M. L. G. Oldfield, A. G. Sheard, Developments in instrumentation and processing for transient heat transfer measurement in a full-stage model turbine, *Journal of Turbomachinery* 111 (1989) 20–27.
 - [31] S. J. Thorpe, S. Yoshino, R. W. Ainsworth, Fabrication and calibration techniques for turbine rotor tip heat transfer gauges, in: Proceedings of the XV Symposium on Measuring Techniques for Transonic and Supersonic Flows in Cascades and Turbomachines, Florence, Italy, 2000.
 - [32] S. J. Thorpe, S. Yoshino, R. W. Ainsworth, N. W. Harvey, Improved fast-response heat transfer instrumentation for short-duration wind tunnels, *Measurement Science and Technology* 15 (2004) 1897–1909.
 - [33] R. W. Ainsworth, A. J. Dietz, T. A. Nunn, The use of semi-conductor sensors for blade surface pressure measurement in a model turbine stage, *Journal of Engineering for Gas Turbines and Power* 113 (1991) 261–268.
 - [34] S. J. Thorpe, S. Yoshino, G. A. Thomas, R. W. Ainsworth, N. W. Harvey, Blade-tip heat transfer in a transonic turbine, *Proceedings of the Institution of Mechanical Engineers, Part A: Journal of Power and Energy* 219 (2005) 421–430.
 - [35] R. W. Ainsworth, R. J. Miller, R. W. Moss, S. J. Thorpe, Unsteady pressure measurement, *Measurement Science and Technology* 11 (7) (2000) 1055–1076.
 - [36] A. P. S. Wheeler, R. D. Sandberg, Direct numerical simulation of a transonic tip flow with freestream disturbances, in: Proceedings of the ASME 2013 Turbine Blade Tip Symposium. TBTS2013. September 30 – October 3, 2013, Hamburg, Germany, no. TBTS2013-2037, 2013.
 - [37] Z. Schabowski, H. Hodson, D. Giacche, B. Power, M. R. Stokes, Aeromechanical optimization of a winglet-squealer tip for an axial turbine, *Journal of Turbomachinery* 136 (2014) 071004.
 - [38] A. S. Virdi, Q. Zhang, L. He, H. D. Li, R. Hunsley, Aerothermal performance of shroudless turbine blade tips with relative casing movement effects, *Journal of Propulsion and Power* 31 (2) (2015) 527–536.
 - [39] A. G. Sheard, Aerodynamic and mechanical performance of a high pressure turbine stage in a transient wind tunnel, Ph.D. thesis, Oxford University (1989).
 - [40] R. J. Miller, An investigation into the unsteady blade row interaction in a one and a half stage axial flow turbine, Ph.D. thesis, Oxford University (1998).